ground water

Methods Note/

NAPL Source Zone Depletion Model and Its Application to Railroad-Tank-Car Spills

by Amanda Marruffo[1], Hongkyu Yoon[2], David J. Schaeffer[3], Christopher P. L. Barkan[1], Mohd Rapik Saat[1], and Charles J. Werth[1]

Abstract

We developed a new semi-analytical source zone depletion model (SZDM) for multicomponent light nonaqueous phase liquids (LNAPLs) and incorporated this into an existing screening model for estimating cleanup times for chemical spills from railroad tank cars that previously considered only single-component LNAPLs. Results from the SZDM compare favorably to those from a three-dimensional numerical model, and from another semi-analytical model that does not consider source zone depletion. The model was used to evaluate groundwater contamination and cleanup times for four complex mixtures of concern in the railroad industry. Among the petroleum hydrocarbon mixtures considered, the cleanup time of diesel fuel was much longer than E95, gasoline, and crude oil. This is mainly due to the high fraction of low solubility components in diesel fuel. The results demonstrate that the updated screening model with the newly developed SZDM is computationally efficient, and provides valuable comparisons of cleanup times that can be used in assessing the health and financial risk associated with chemical mixture spills from railroad-tank-car accidents.

Introduction

The release of lighter than water nonaqueous phase liquids (LNAPLs) to the subsurface causes soil and groundwater contamination, giving rise to environmental and health risks (ATSDR 1999). A notable example is hazardous chemical spills by railroad tank cars (BOE 2009); and many of these spills have involved organic chemical mixtures such as gasoline, jet fuel, crude oil, diesel fuel, and various ethanol-fuel blends. A number of chemical spill sites have resulted in long cleanup times for soil and groundwater and high costs, which call into question whether some LNAPLs should be shipped in more robust tank cars, or whether pricing structures for shipping LNAPLs adequately represent the economic risk of chemical spills. To assess the environmental risk of soil and groundwater contamination due to railroad-tank-car spills, a screening model for single-component LNAPLs was developed to predict contaminant migration in soil and groundwater, cleanup times, and cleanup costs (Yoon et al. 2009). There is a pressing need to develop a similar screening model for NAPL mixtures including LNAPLs commonly shipped by railroad to evaluate environmental risk more comprehensively.

Many studies have evaluated NAPL source zone depletion in groundwater (Ruiz-Aguilar et al. 2003). Field sites are typically heterogeneous, and NAPL is nonuniformly distributed. As a result, distinguishing the mechanisms that control NAPL source zone depletion is often not possible, and upscaled first-order mass transfer coefficients are used. Several first-order mass transfer coefficients have been developed to describe NAPL mass

[1]Department of Civil and Environmental Engineering, University of Illinois at Urbana-Champaign, 205 N. Mathews Ave., Urbana, IL 61801.

[2]Corresponding author: Department of Geomechanics, Sandia National Laboratories, P.O. Box 5800, MS 0735, Albuquerque, NM 87185-0735; (505) 284-3609; fax: (505) 844-7354; hyoon@sandia.gov

[3]Department of Veterinary Biosciences, University of Illinois at Urbana-Champaign, Urbana, IL.

Received February 2011, accepted July 2011.

doi: 10.1111/j.1745-6584.2011.00863.x

transfer to groundwater, and these are a function of NAPL mass remaining and several site-specific fitting parameters (Parker and Park 2004; Christ et al. 2006; Zhang et al. 2008) that depend on the distribution and morphology of NAPL, and the distribution of permeability. Existing upscaled mass transfer expressions have only been developed for single-component NAPLs; they cannot be easily extended to multicomponent NAPLs because they do not account for the mole fraction of NAPL components in a mixture or potential cosolvent effects.

Another approach to describe NAPL mass transfer to groundwater has been to develop simplified analytical or semi-analytical models that assume NAPL is locally in equilibrium with pore water, and dissolution is limited by advection and dispersion of pore water away from the NAPL source (Huntley and Beckett 2002; Falta 2003; Peter et al. 2008; Yoon et al. 2009). The advective flux term is a function of relative permeability, which depends on NAPL saturation, and the dispersive flux term accounts for NAPL mass transfer to adjacent pore water (Hunt et al. 1988). These models have primarily been used to model source zone depletion of single-component NAPLs (Falta 2003; Yoon et al. 2009); for multicomponent NAPLs, source zone depletion has not been considered (Huntley and Beckett 2002; Hansen and Kueper 2007; Peter et al. 2008). There is a need to extend these semi-analytical models to consider multicomponent NAPLs including similar mixtures (e.g., petroleum hydrocarbon and chlorinated organic mixtures) and dissimilar mixtures (e.g., ethanol blended gasoline), and to incorporate other mass removal mechanisms such as volatilization to the overlying soil, particularly, for LNAPLs that are trapped near capillary fringe.

The objectives of this work are to develop a new semi-analytical source zone depletion model (SZDM) for multicomponent LNAPLs (i.e., mixture), and to incorporate this into the Hazardous Materials Transportation Environmental Consequence Model (HMTECM). The HMTECM was developed to predict the relative impact of single-component LNAPLs released from railroad-tank-car accidents on soil and groundwater contamination and cleanup times (Yoon et al. 2009). The newly developed SZDM will first be tested by comparing results to those from a numerical model, and from another semi-analytical model that does not consider source zone depletion. The updated HMTECM will then be used to predict groundwater contamination and cleanup times for complex mixtures of concern in the railroad industry, that is, gasoline, diesel fuel, crude oil, and E95. Although the SZDM is not limited to any specific type of spill, we focus on LNAPL problems related to railroad-tank-car spills as a practical example.

SZDM for a Multicomponent LNAPL

The new SZDM considers a three-dimensional (3D) LNAPL lens that shrinks over time as mass partitions to the aqueous and gas phases. The aqueous concentration of each component within the LNAPL source zone is assumed to be in equilibrium locally with the LNAPL phase. For similar compounds in a mixture (such as petroleum hydrocarbons in gasoline), the activity coefficients are assumed to be unity (Corseuil et al. 2004). In the absence of a cosolvent, the solubility of mixture component i in water ($C^{\mathrm{m}}_{\mathrm{w},i}$) is calculated according to Raoult's law (Weber and DiGiano 1996). The gas concentration of each component within the NAPL source zone is also assumed to be in equilibrium locally with the LNAPL phase, and the vapor-phase form of Raoult's law is similarly used. In the presence of a cosolvent (e.g., ethanol), the linear/log-linear model modified by Heermann and Powers (1998) was incorporated into the HMTECM to estimate solubility enhancement.

In our previous SZDM for pure LNAPLs, the source zone was discretized to account for mass depletion in each cell (Yoon et al. 2009). In our new model, we assume that all components of a mixture are ideally mixed within the source zone. This implies that spatial variations of LNAPL are not considered. This assumption allows us to use a relatively simple and computationally efficient analytical solution to account for transient LNAPL dissolution over time, which allows for incorporation of any number of mixture components. We initially considered using a numerical scheme and accounting for the mass depletion in each cell, but this was deemed too computationally demanding for a screening model. Full details of the analytical equations used to describe multicomponent LNAPL dissolution are reported in the literature (Huntley and Beckett 2002; Peter et al. 2008; Yoon et al. 2009), so only equations for each flux term from the source zone are summarized here. The unique aspects of our model are combining these equations with a vapor flux term, and accounting for source zone size depletion over time.

1. The advective flux of a compound through the LNAPL source (lens and residual), $J_{\mathrm{adv},i}$, is the product of the water specific discharge (q_{w}) and the effective solubility of a component i ($C^{\mathrm{eff}}_{\mathrm{w},i}$):

$$J_{\mathrm{adv},i} = q_{\mathrm{w}} C^{\mathrm{eff}}_{\mathrm{w},i}. \tag{1}$$

The groundwater specific discharge varies as a function of water saturation (i.e., 1-NAPL saturation)

$$q_{\mathrm{w}} = -\frac{k_{\mathrm{rw}} k \rho_{\mathrm{w}} g}{\mu_{\mathrm{w}}} i, \tag{2}$$

where k_{rw} is the water relative permeability, k is the intrinsic permeability of the soil, ρ_{w} is the water density, g is the gravitational constant, μ_{w} is the water viscosity, and i is the hydraulic gradient. Dispersion through the NAPL source zone can be neglected due to local equilibrium within the NAPL source zone (Seagren et al. 1999; Yoon et al. 2009).

2. The dispersive flux from the z direction (i.e., the bottom of the source zone) with clean water coming into the source zone (Hunt et al. 1988) is expressed as

$$J_{\mathrm{disp\_}z,i} = C^{\mathrm{eff}}_{\mathrm{w},i} \theta \sqrt{4 D_{\mathrm{t},i} v_x / (\pi L_x)}, \tag{3}$$

where θ is the porosity, $D_{t,i}$ is the transverse dispersion coefficient, v_x is the water pore velocity, and L_x is the horizontal distance along the NAPL source zone. The same approach is used in the y direction. The hydrodynamic dispersion coefficient is given by

$$D_{t,i} = D_{\text{eff},i} + v_x \alpha_t, \tag{4}$$

where $D_{\text{eff},i}$ is the effective diffusion coefficient of compound i in water and α_t is the transverse dispersivity in the z direction. The effective diffusion coefficient is the product of the tortuosity, which is simply porosity in this study, and the aqueous diffusion coefficient (Grathwohl 1998). The transverse dispersivity in the NAPL source zone, which is generally much smaller than that in the groundwater plume, can be obtained from available field-scale experimental data (Eberhardt and Grathwohl 2002; Klenk and Grathwohl 2002; Cirpka et al. 2006).

3. The vapor diffusive flux accounts for LNAPL volatilization from the LNAPL lens, and is described using Fick's first law for steady-state vapor transport toward the ground surface with a zero concentration boundary

$$J_{v,i} = -D_{\text{veff},i} \frac{dC_{g,i}}{dz} = D_{\text{veff},i} \frac{C_{\text{vsat},i}}{Z_{\text{depth}}}, \tag{5}$$

where $J_{v,i}$ is the vapor diffusive flux of a compound i from the top of the LNAPL to the ground surface, $D_{\text{veff},i}$ is the effective vapor diffusion coefficient, $C_{\text{vsat},i}$ is the saturated gas concentration, and Z_{depth} is the distance from the top of the LNAPL to the ground surface. $D_{\text{veff},i}$ is computed using the Millington and Quirk (1961) equation.

4. Total mass removal over the time interval (dt) from these processes can be summed

$$M_{\text{removal},i} = [J_{\text{adv},i}(L_y L_z) + J_{\text{disp\_}z,i}(L_x L_y) + 2 \times J_{\text{disp\_}y,i}(L_x L_z) + J_{v,i}(L_x L_y)]dt, \tag{6}$$

where L_y and L_z are the width and depth of the LNAPL source zone and a factor of two in front of $J_{\text{disp\_}y,i}$ is due to the symmetrical geometry of the source zone in the y direction.

Per Equation (6), the advective, dispersive, and vapor mass fluxes are proportional to the cross-sectional area for each flux component. As the source zone size decreases over time, the fluxes decrease proportionally. This concept is incorporated into the four components of volumetric flux from the source zone. The source zone length (L_x) is reduced by the advective flux in the x direction, the source zone width (L_y) by the dispersive flux in the y direction, and the source zone depth (L_z) by the dispersive flux and vapor diffusive flux in the z direction. Time-dependent source zone lengths in the SZDM are expressed as

$$L_x(t+1) = L_x(t)\left(1 - \frac{\sum_i J_{\text{adv},i}(L_y(t)L_z(t))dt/\rho_i}{V_{\text{NAPL}}(t)}\right) \tag{7}$$

$$L_y(t+1) = L_y(t)\left(1 - \frac{\sum_i J_{\text{disp\_}y,i}(L_x(t)L_z(t))dt/\rho_i}{V_{\text{NAPL}}(t)}\right) \tag{8}$$

$$L_z(t+1) = L_z(t)\left(1 - \frac{\sum_i (J_{\text{disp\_}z,i} + J_{v,i})(L_x(t)L_y(t))dt/\rho_i}{V_{\text{NAPL}}(t)}\right) \tag{9}$$

where L_i is the dimension of the source zone in the i direction, dt is the time interval between t and $t+1$, ρ is the density of each component, and $V_{\text{NAPL}}(t)$ is the NAPL volume within the source zone at time t.

SZDM Validation

Results from the SZDM are compared to those from a numerical model and from a semi-analytical model without source zone depletion. The numerical model developed by Frind et al. (1999) was implemented in this study, and it considers 3D advection and dispersion, and first-order NAPL dissolution. It was successfully tested against a one-dimensional analytical dissolution model (Powers et al. 1992) and published field-scale data (Frind et al. 1999) (results not shown). The semi-analytical model developed by Huntley and Beckett (2002) was used for comparison. It employs the steady-state dispersion equation for NAPL dissolution from the source zone to surrounding groundwater (Hunt et al. 1988), and the change in effective solubility of each component in a mixture due to dissolution. It will be referred to as the source zone constant model (SZCM) in this work.

Mixture composition from a field site experiment (Frind et al. 1999) was used to create two different example cases for model comparisons. A first-order dissolution rate (3.0/d) calibrated to the laboratory and field data in Frind et al. (1999) was used. As the value of the dissolution rate is large, it is not far from the equilibrium condition (Frind et al. 1999). Hence, the local equilibrium assumption employed by the SZDM will be shown to be adequate. The example mixture contained trichloromethane (TCM), trichloroethylene (TCE), and perchloroethylene (PCE). The solubility and initial mole fraction (in parenthesis) of these three components are 8760 mg/L (0.078), 1270 mg/L (0.439), and 242 mg/L (0.483), respectively. The two cases each contained a 1.5-m long, 0.3-m wide, by 0.1-m deep source zone. In Cases 1 and 2, the source zone was uniformly contaminated with the NAPL mixture at residual saturation (0.06) and a NAPL pool with a saturation of 0.3, respectively, and groundwater velocity was 0.00864 and 0.0864 m/d, respectively. In both cases, porosity was 0.333 and horizontal and vertical dispersivities in the source zone were 2.5 and 1 cm, respectively. The Burdine relative permeability function was used to calculate water velocity in the source zone. Clean water was flushed through the domain in each case. The numerical grid consisted of grid blocks 0.1-m long, 0.05-m wide, by 0.02-m tall, and the numerical domain was 1.5-m long, 3-m wide, by 1.5-m deep.

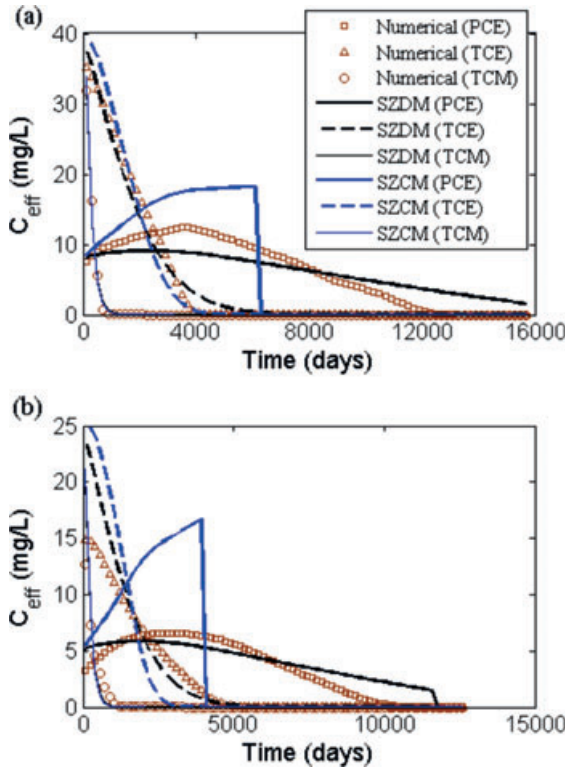

Figure 1. Comparison of effluent concentrations for (a) Case 1 and (b) Case 2. The SZDM, a numerical model, and the SZCM are compared.

The results for Cases 1 and 2 are shown in Figure 1. For Case 1 (Figure 1a), both the SZDM and SZCM results coincide with those for the numerical model for the highest solubility compound (TCM). For the intermediate and low solubility compounds (TCE and PCE, respectively), the SZDM and numerical model results are similar, and differences in time to reach 10% of the initial effluent concentration or mass remaining are generally within 20%. The SZCM and numerical model results are also similar for the intermediate solubility compound (TCE), with differences in the time to reach 10% of the initial effluent concentration (C_{eff}) or mass remaining less than 18%. However, the SZCM does a poor job of matching SZDM and numerical model results for the lowest solubility compound. This is most evident after TCE is completely removed, resulting in a much shorter removal time. This is mainly due to the constant source zone size with decreasing LNAPL saturation in the SZCM. For example, if the length of the source zone in each direction is reduced by 25%, the mass removal rates (Equation 6) from the dispersive flux, advective flux, and diffusive flux in the SZDM are 35, 44, and 44% lower than those in the SZCM, respectively, resulting in faster removal with the SZCM.

For Case 2 (Figure 1b), differences in time to reach 10% of the initial mass remaining between the SZDM and numerical model results are within 24%. Hence, the SZDM and numerical model profiles are similar but show slightly more discrepancy than for the lower NAPL saturation case (Case 1). This is mainly because NAPL composition and saturation are averaged spatially in the SZDM. As NAPL saturation in the source zone increases, NAPL along the boundary of the source zone is removed faster over time in the numerical model. However, NAPL saturation in the SZDM is averaged over the source zone, resulting in less advective flux compared to the numerical model. As in Case 1, the SZCM did not match the PCE concentration profile. Given that there is no fitting parameter in the SZDM and transverse dispersion coefficients were the same for both models, we propose that the errors in cleanup time are adequately small for a screening model and the computationally efficient SZDM adequately captures the overall removal kinetics and source zone longevity predicted by the numerical model.

Modified HMTECM Results for Hydrocarbon Mixtures

The SZDM was added to the groundwater module of the HMTECM and the details of the updated HMTECM are presented in the Supporting Information (Appendix S1 and Figure S1). The updated HMTECM was used to demonstrate the effects of chemical properties on cleanup time; four hydrocarbon mixtures tested are gasoline, diesel fuel, crude oil, and E95. Key properties of the individual components and groups within the mixtures are shown in Table S1, Supporting Information. The benzene, toluene, ethylbenzene, and xylenes (BTEX) components of all mixtures were separately tracked because of their adverse impact on health and low maximum contaminant level values. The remaining components in gasoline were categorized into 11 groups for alkanes, alkenes, and high molecular weight compounds based on Foster et al. (2005). The remaining components in diesel fuel and crude oil were categorized into five groups based on chemical structure. Although there is very little computational burden on the number of components in a mixture, the use of groups allows us to analyze the results more easily, for example, determine what class of compounds limits cleanup. The density, vapor pressure, and diffusion coefficient for each group were calculated using a simple linear mixing rule based on the mole fraction of each component in a group (Huntley and Beckett 2002; Foster et al. 2005). Except for E95, the same approach was used for calculating aqueous solubility. The linear/log-linear model was used to calculate the solubility for E95.

Three soil types were evaluated: coarse sand, fine sand, and silt. The hydrogeologic properties, transport parameters, and system parameters for these are given in Table 1. The soil module of the HMTECM was used to simulate four different chemical spill volumes for gasoline: 13.82, 49.64, and 89.35 m^3. These spill volumes were chosen to represent 12.5, 50, and 90% of a railroad-tank-car volume (99.3 m^3). The approximate thicknesses of the LNAPL lens and residual zone were 0.1 to 0.2 and 0.5 to 1.5 m, respectively. As previously described in Yoon et al. (2009), the LNAPL lens and residual zone were approximated as different size rectangular boxes based on LNAPL distributions that result from the soil

Table 1
Soil Properties Used in Simulations and Spill Conditions

Physical Properties	Coarse Sand	Fine Sand	Silt
Hydraulic conductivity (m/d)	50	7	1
Hydraulic gradient	0.006	0.006	0.006
Lens NAPL saturation	0.35	0.35	0.35
Effective porosity	0.42	0.33	0.33
Horizontal transverse dispersivity in the NAPL source (m)	0.05	0.05	0.05
Vertical transverse dispersivity in the NAPL source (m)	0.025	0.025	0.025
Longitudinal dispersivity in groundwater plume (m)	1	1	1
Transverse dispersivity in groundwater plume (m)	0.1	0.1	0.1

Notes: To construct the initial NAPL distribution, depth to groundwater was 3 m, maximum volume of spill was 94.6 m^3, and spill duration was 12 h. Aquifer thickness was 10 m. Cleanup criteria include total petroleum hydrocarbons (TPH)-soil (5000 mg/kg), TPH-water (1 mg/L), and maximum contaminant levels for BTEX (0.005, 2, 0.1, and 0.7 mg/L). Remediation time when the pumping system began was 30 d after spill event. Pumping rates for hydrocarbons (gasoline, diesel, and crude oil) and cosolvents (E95) are 100 and 10 m^3/d, respectively.

module. The initial LNAPL distributions for gasoline were used for other mixtures to facilitate comparison of contaminant migration and cleanup among different chemical mixtures.

Cleanup times for the four mixtures are shown in Figure 2. As previously noted, the initial LNAPL distribution is the same for all mixtures in each soil type. Average solubility values of mixtures decrease from E95, to gasoline, crude oil, and diesel fuel. Cleanup time is inversely proportional to average solubility values. This results in cleanup times as short as 20 d for E95, and as long as 62,288 d for diesel fuel. Although E95 has the shortest cleanup time, there are some negative implications. Ethanol increases the solubility of hydrocarbons in the gasoline mixture. This results in greater concentrations of BTEX (as well as other hydrocarbons) and extended downgradient contamination in groundwater before pumping begins; hence, more pumping wells are required for E95 than for other mixtures to remove the contaminated groundwater plume. Diesel fuel has the smallest mole fraction of BTEX, which accounts for the highest solubility compounds in gasoline, and has no groups with solubility more than 100 mg/L; in contrast, gasoline has four groups with solubility more than 100 mg/L. The two highest solubility groups in diesel fuel are approximately two orders of magnitude smaller than the two highest solubility groups in crude oil because more individual components with greater solubility are included in the composition of crude oil. This explains why diesel fuel has a much longer cleanup time than other mixtures.

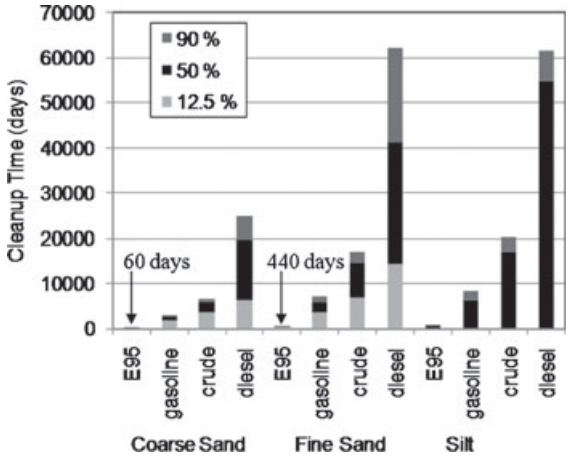

Figure 2. Cleanup time of E95, gasoline, diesel fuel, and crude oil for four difference spill volumes in coarse sand, fine sand, and silt. A percent spill represents the percent of a tank volume of 99.3 m^3, a size typical of tank cars used for many NAPL mixtures.

Soil permeability decreases from the coarse sand, to the fine sand and the silt. Cleanup times increase as soil permeability decreases for the same amount of NAPL in the source zone. For example, cleanup times for diesel fuel, 50% spill, in coarse sand, fine sand, and silt are 19,780, 41,420, and 54,820 d, respectively. Different LNAPL volumes reach groundwater for the different soil types. For example, less LNAPL reaches the groundwater table in silt because it has the lowest permeability. In fact, no LNAPL reaches the groundwater for spill volumes less than 50% in silt. Consequently, cleanup times for silt are only shown for the 50 and 90% spill volumes. For the 50% spill volume case, approximately 60% less NAPL reaches groundwater in silt than in coarse sand, but silt cleanup times are 2000 d longer due to slower mass removal rate in the low permeability soil.

Conclusion

The newly developed semi-analytical SZDM was tested against a 3D numerical model for several different conditions with adequate results. The SZDM was added to the groundwater module (i.e., accounts for NAPL dissolution, NAPL volatilization, and contaminant transport in groundwater) of the HMTECM, a screening model for prediction of subsurface contamination and cleanup times for LNAPLs released from railroad-tank-car accidents. The updated HMTECM was used to assess the influence of chemical properties, soil permeability, and spill volume on cleanup times of four mixtures commonly shipped by railroad tank cars.

Cleanup times for the mixtures (E95, gasoline, crude oil, and diesel fuel) in three different soil types with a 3-m depth to groundwater were evaluated. The solubility of the individual components within the mixture has the greatest impact on cleanup time. For example, the highest solubility mixture, E95, had the shortest cleanup time. Cleanup times generally increased as soil permeability decreased for the same amount of NAPL in the source zone, due to lower groundwater flow. Cleanup times generally increased with more LNAPL spilled in the same soil type, due to a larger fraction of LNAPL reaching groundwater.

To improve on the HMTECM, it is advised to integrate biodegradation and natural attenuation of contaminants because these remediation processes are especially important for petroleum hydrocarbons. This integration will help in estimating more accurate cleanup times. In addition, other remediation options can be used, such as in situ air sparging, along with pump and treat or as an alternative method.

Acknowledgments

This research was sponsored by the Association of American Railroads. The authors are grateful to Robert Fronczak and the AAR for their support and assistance. Sandia National Laboratories is a multiprogram laboratory managed and operated by Sandia Corporation, a wholly owned subsidiary of Lockheed Martin Corporation, for the U.S. Department of Energy's National Nuclear Security Administration under contract DE-AC04-94AL85000.

Supporting Information

Additional Supporting Information may be found in the online version of this article:

Appendix S1. Update of HMTECM.

Table S1. Individual component properties found in gasoline, diesel fuel, crude oil, and E95.

Figure S1. Schematic of NAPL source zone, groundwater plume zone, and pumping systems in HMTECM. Comparison of the modified Domenico model and Wexler's solution is shown.

Please note: Wiley-Blackwell is not responsible for the content or functionality of any supporting information supplied by the authors. Any queries (other than missing material) should be directed to the corresponding author for the article.

References

Agency for Toxic Substances and Disease Registry (ATSDR). 1999. *Toxicological Profile for Total Petroleum Hydrocarbons (TPH).* Atlanta, Georgia: U.S. Department of Health and Human Services, Public Health Service.

Bureau of Explosives (BOE). 2009. Annual Report of Hazardous Materials Transported by Rail: Calendar Year: 2008. Report BOE 08-1. Pueblo, Colorado: Association of American Railroads.

Christ, J.A., C.A. Ramsburg, K.D. Pennell, and L.M. Abriola. 2006. Estimating mass discharge from dense nonaqueous phase liquid source zones using upscaled mass transfer coefficients: An evaluation using multiphase numerical simulations. *Water Resources Research* 42, no. 11: W11420.

Cirpka, O.A., A. Olsson, Q.S. Ju, M.A. Rahman, and P. Grathwohl. 2006. Determination of transverse dispersion coefficients from reactive plume lengths. *Ground Water* 44, no. 2: 212–221.

Corseuil, H.X., B.I.A. Kaipper, and M. Fernandes. 2004. Cosolvency effect in subsurface systems contaminated with petroleum hydrocarbons and ethanol. *Water Research* 38, no. 6: 1449–1456.

Eberhardt, C., and P. Grathwohl. 2002. Time scales of pollutants dissolution from complex organic mixtures: Blobs and pools. *Journal of Contaminant Hydrology* 59, no. 1–2: 45–66.

Falta, R.W. 2003. Modeling sub-grid-block-scale dense nonaqueous phase liquid (DNAPL) pool dissolution using a dual-domain approach. *Water Resources Research* 39, no. 12: 1360–1368.

Foster, K.L., D. Mackay, T.F. Parkerton, E. Webster, and L. Milford. 2005. Five-stage environmental exposure assessment strategy for mixtures: Gasoline as a case study. *Environmental Science and Technology* 39, no. 8: 2711–2718.

Frind, E.O., J.W. Molson, M. Schirmer, and N. Guiguer. 1999. Dissolution and mass transfer of multiple organics under field conditions: The Borden emplaced source. *Water Resources Research* 35, no. 3: 683–694.

Grathwohl, P. 1998. *Diffusion in Natural Porous Media: Contaminant Transport, Sorption/Desorption and Dissolution Kinetics.* Boston, Massachusetts: Kluwer Academic Publishers.

Hansen, S.K., and B.H. Kueper. 2007. An analytical solution to multi-component NAPL dissolution equations. *Advances in Water Resources* 30, no. 3: 382–388.

Heermann, S.E., and S.E. Powers. 1998. Modeling the partitioning of BTEX in water-reformulated gasoline systems containing ethanol. *Journal of Contaminant Hydrology* 34, no. 4: 315–341.

Hunt, J.R., N. Sitar, and K.S. Udell. 1988. Non-aqueous phase liquid transport and cleanup: Analysis of mechanisms. *Water Resources Research* 24, no. 8: 1247–1258.

Huntley, D., and G.D. Beckett. 2002. Persistence of LNAPL source: Relationship between risk reduction and LNAPL recovery. *Journal of Contaminant Hydrology* 59, no. 1–2: 3–26.

Klenk, I.D., and P. Grathwohl. 2002. Transverse vertical dispersion in groundwater and the capillary fringe. *Journal of Contaminant Hydrology* 58, no. 1–2: 111–128.

Millington, R., and J. Quirk. 1961. Permeability of porous solids. *Transactions of the Faraday Society* 57: 1200–1207.

Parker, J.C., and E. Park. 2004. Modeling field-scale dense nonaqueous phase liquid dissolution kinetics in heterogeneous aquifers. *Water Resourcse Research* 40, no. 5: W05109.

Peter, A., B. Miles, and G. Teutsch. 2008. Estimation of emission from an LNAPL contaminated zone considering groundwater recharge. *Journal of Environmental Geology* 55, no. 2: 321–337.

Powers, S.E., L.M. Abriola, and W.J. Weber. 1992. An experimental investigation of nonaqueous phase liquid dissolution in saturated subsurface systems: Steady state mass transfer rates. *Water Resources Research* 28, no. 10: 2691–2705.

Ruiz-Aguilar, G.M.L., K. O'Reilly, and P.J.J. Alvarez. 2003. A comparison of benzene and toluene plume lengths for sites contaminated with regular vs. ethanol-amended gasoline. *Ground Water Monitoring and Remediation* 23, no. 1: 48–53.

Seagren, E.A., B.E. Rittman, and A.J. Valocchi. 1999. A critical evaluation of the local equilibrium assumption in modeling of NAPL-pool dissolution. *Journal of Contaminant Hydrology* 39, no. 1–2: 109–135.

Weber, W.J., and F.A. DiGiano. 1996. *Process Dynamics in Environmental Systems.* New York: Wiley-Interscience, John Wiley & Sons Inc.

Yoon, H., C.J. Werth, C.P.L. Barkan, D.J. Schaeffer, and P. Anand. 2009. An environmental screening model to assess the consequences to soil and groundwater from railroad-tank-car spills of light non-aqueous phase liquids. *Journal of Hazardous Materials* 165, no. 1–3: 332–344.

Zhang, C., H. Yoon, C.J. Werth, A.J. Valocchi, N.B. Basu, and J.W. Jawitz. 2008. Evaluation of simplified mass transfer models to simulate the impacts of source zone architecture on nonaqueous phase liquid dissolution in heterogeneous porous media. *Journal of Contaminant Hydrology* 102, no. 1–2: 49–60.